



**HAL**  
open science

# AMORPHOUS SOLIDS: A REVIEW OF THE APPLICATIONS OF THE MÖSSBAUER EFFECT

J. Coey

► **To cite this version:**

J. Coey. AMORPHOUS SOLIDS: A REVIEW OF THE APPLICATIONS OF THE MÖSSBAUER EFFECT. Journal de Physique Colloques, 1974, 35 (C6), pp.C6-89-C6-105. 10.1051/jphyscol:1974608 . jpa-00215708

**HAL Id: jpa-00215708**

**<https://hal.science/jpa-00215708>**

Submitted on 4 Feb 2008

**HAL** is a multi-disciplinary open access archive for the deposit and dissemination of scientific research documents, whether they are published or not. The documents may come from teaching and research institutions in France or abroad, or from public or private research centers.

L'archive ouverte pluridisciplinaire **HAL**, est destinée au dépôt et à la diffusion de documents scientifiques de niveau recherche, publiés ou non, émanant des établissements d'enseignement et de recherche français ou étrangers, des laboratoires publics ou privés.

## AMORPHOUS SOLIDS : A REVIEW OF THE APPLICATIONS OF THE MÖSSBAUER EFFECT

J. M. D. COEY

Groupe des Transitions de Phases, Centre National de la Recherche Scientifique  
B. P. 166, 38042 Grenoble-Cedex, France

**Résumé.** — L'effet Mössbauer a été beaucoup utilisé dans l'étude de la structure et des liaisons d'oxydes et chalcogènes vitreux, notamment ceux contenant du fer, de l'étain, du tellure et de l'antimoine. Le comportement magnétique d'alliages et de composés de fer amorphes ainsi que la transition vitreuse ont aussi fait l'objet de quelques études. Tout d'abord nous introduisons quelques idées élémentaires sur les solides amorphes. Ensuite nous exposons les résultats obtenus par spectroscopie Mössbauer concernant la structure, les liaisons et le magnétisme dans ces solides. Finalement nous analysons les possibilités présentes et futures de cette technique appliquée aux solides amorphes.

**Abstract.** — The Mössbauer effect has been used intensively to help investigate the structure and bonding of oxide and chalcogenide glasses, particularly those containing iron, tin, tellurium and antimony. Both the properties of magnetically ordered amorphous iron compounds and alloys and the glass transition have also been examined. After an introduction to some elementary ideas of amorphous solids, the information obtained from the Mössbauer studies of their structure, bonding and magnetic properties is reviewed. An attempt is made to assess both the scope of the technique and its future prospects in this field.

Amorphous solids are of growing interest to theoretical physicists and materials scientists. Much of the impetus for these studies is due to the technical applications of amorphous semiconductors, but the theoretical and experimental problem of recovering solid state physics without the periodic lattice is also of very great interest.

The textbook definition of an amorphous solid is one in which three dimensional periodicity is absent [1]. A solid may be arbitrarily defined as having a viscosity greater than  $10^{14.6}$  poise so that it takes at least a day to respond to a small impressed shear stress [2]. These definitions apply to a considerable fraction of all the materials which have ever been studied using the Mössbauer effect, ranging from noncrystalline elements, compounds and alloys to impurities in crystalline hosts, disordered alloys and even surfaces. As it would be an impossible task to cover all the work, this paper is mainly restricted to those solids which have no semblance of a periodic lattice.

A review with similar scope was given recently by Kalvius [3]. Ruby [4] has written a brief critical survey of the applicability of Mössbauer spectroscopy to the study of supercooled liquids and glasses, and another review, mainly devoted to the semiconducting glasses, appeared last year [5]. Kurkjian's review of the oxide glasses [6] covers the earlier results and includes an introduction to the Mössbauer effect. Work on the related topics of dilute and disordered alloys and impurity studies is reported elsewhere in these proceedings. Frozen solutions [7], surfaces and fine par-

ticles [8] and magnetic dead layers [9] have all been reviewed within the last few years. A new book [10] serves as a good introduction to the general subject of amorphous and liquid semiconductors, while more details of the structural and electronic [11-13] or magnetic [13, 14] properties of amorphous solids may be had from other recent conference proceedings.

In this article, some elementary ideas of amorphous solids will first be introduced, followed by a survey of the information which has been obtained about their structure and bonding and their magnetic properties using Mössbauer spectroscopy. Finally, conclusions are drawn about the usefulness of the technique in this field.

**1. Introduction to amorphous solids.** — **1.1 PREPARATION.** — There are various ways of obtaining amorphous solids, but the most common are by rapidly cooling the liquid to form a *glass* or by subliming the gas, usually on a cold amorphous substrate if the material is a poor glass former and quenching won't work. Other methods include spluttering by bombardment with inert gas ions, irradiation with energetic neutrons, chemical precipitation from solution, gas phase reactions, electrodeposition and decomposition of gaseous compounds by an rf discharge. Implantation of ions into a matrix of the same element may produce an amorphous surface layer. Massive plastic deformation can also destroy the three-dimensional periodicity of a crystal. It is no surprise that different methods of preparation do not always

result in amorphous solids with the same properties, and hence it is important to characterise the structure as far as possible. The structures of glasses are derived from those of the liquid, but this is not necessarily true of amorphous solids prepared by other methods. For example, vapour deposited silicon is a tetrahedrally-bonded semiconductor, yet the liquid is a dense-packed metal. Furthermore, the structure can be modified by heat treatment which may relax bonds, anneal out defects or segregate different amorphous or crystalline phases.

**1.2 CHARACTERISATION.** — Amorphous materials used to be identified by their conchoidal fracture but this method has been superseded by X-ray, electron or neutron diffraction. If only a few diffuse reflections appear in the diffraction pattern the material is deemed amorphous. With electron microscopy it is also possible to examine the sample directly by transmission, if it is thin enough, or otherwise by making a replica of the surface. In amorphous materials, little texture is evident whereas in crystalline materials the crystallite structure can be clearly seen. Typical results of both measurements are shown in figure 1.

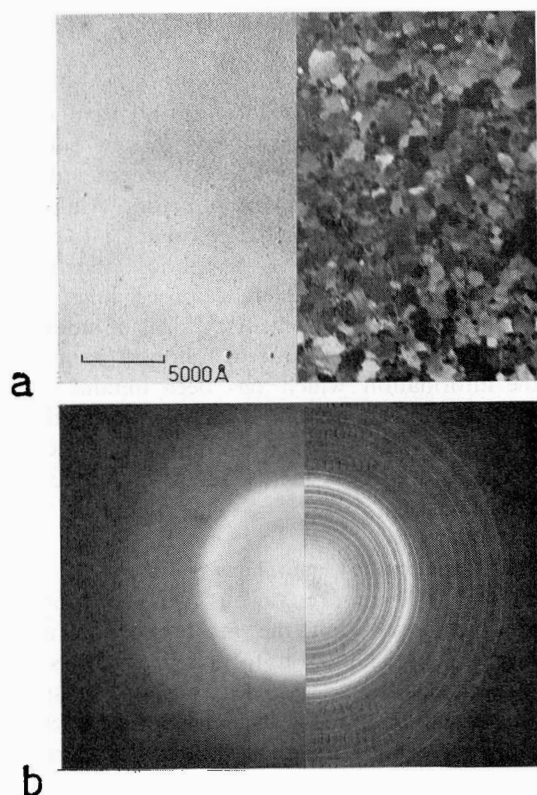


FIG. 1. — *a*) Transmission electron micrographs and *b*) diffraction patterns of a 5 000 Å FeGe film. The amorphous film is shown on the left of each picture and the film after recrystallisation in the electron beam is shown on the right.

Another widely used technique is thermal analysis. The amorphous state of a solid is thermodynamically unstable. A glass forms when a liquid can be super-

cooled sufficiently far below its melting point,  $T_m$ , for the relaxation time towards the crystalline state to be long compared with experimental measuring times. This occurs at  $T_g$ , the glass transition. On reheating the glass, there will be a small increase in the specific heat at  $T_g$ , followed by another small one near  $T_m$ . However, if the material is not a good glass former, recrystallisation of the supercooled liquid may intervene at  $T_c$ ,  $T_g < T_c < T_m$ , giving a large negative peak in the specific heat, followed by a large positive one on melting at  $T_m$ . There is no consensus as to whether the glass transition is a thermodynamic phase transition, or if it is just due to a rapid, but smoothly varying change of relaxation time, like the superparamagnetic blocking transition. In any case, for practical purposes  $T_g$  can be measured to within a few degrees.

Infra-red and Raman spectroscopy may also be used to characterise some amorphous materials as selection rules valid in crystals are relaxed in the amorphous state. Other physical measurements cannot be used to infer *directly* that a substance is amorphous, even though there are often dramatic differences in physical properties compared to the crystalline form.

**1.3 STRUCTURE.** — The structure of amorphous materials has been a subject of controversy ever since the random-network [15] and microcrystallite [16] models for silicate glasses were proposed forty years ago. The problem is to properly reconcile the relatively high degree of short-range order evidenced by the diffuse rings in the diffraction pattern with the absence of long range order. As amorphous solids exist which exhibit every type of chemical bonding from van der Waal's to metallic it is impossible for one prototype structure to apply to them all. In fact it is quite difficult to determine the structure of even one material because the information contained in the normal diffraction pattern is incomplete. All that can be derived from the diffraction pattern is a *radial* distribution function such as  $F(r)$  where  $F(r) dr = 4 \pi r^2 \rho_a(r) dr$  is the probability of finding an atom within  $r$  and  $r + dr$  of any given atom;  $\rho_a(r)$  is the local atomic density. Another frequently used function is the differential radial distribution function  $\Delta F(r) = 4 \pi r^2 (\rho_a(r) - \rho_0)$  where  $\rho_0$  is the mean atomic density.  $F(r)$  is quadratic at large distances whereas  $\Delta F(r)$  tends to zero

$$\Delta F(r) = 8 \pi r \int_0^\infty s \left( \frac{I(s)}{Nf^2} - 1 \right) \sin 2 \pi r s ds \quad (1)$$

where  $s$  is the magnitude of the scattering vector  $2 \sin \theta / \lambda$ ,  $N$  is the number of scattering atoms and  $f$  is the atomic scattering factor, supposing that the solid is monatomic. The observed diffracted intensity  $I(s)$  has been normalised and corrected for such things as geometrical and thermal effects and Compton scattering. To reduce spurious structure in  $\Delta F(r)$  due to truncation errors,  $I(s)$  should be measured out to the largest possible values of  $s$ . A typical radial distribution function is shown in figure 2. The coordination number

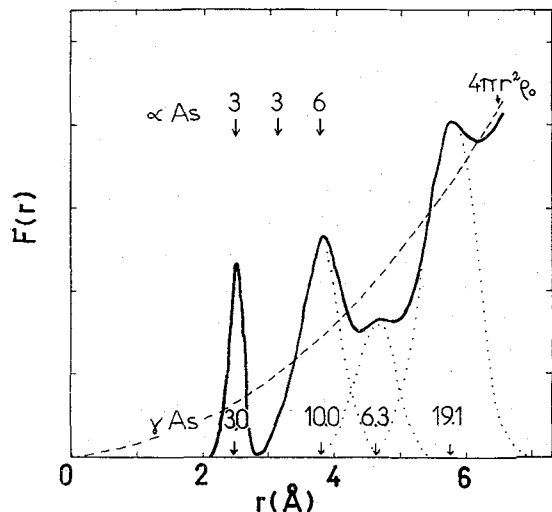


FIG. 2. — The radial distribution function for amorphous ( $\gamma$ ) Arsenic. The dotted line shows the decomposition into peaks corresponding to the first four shells of neighbours, and the numbers of atoms in each are marked. The positions of the first three sets of neighbours in crystalline ( $\alpha$ ) Arsenic are shown for comparison (from ref. [17]).

of arsenic is derived from the area of the first peak, and is the same as in the crystal. Differences begin to appear from the second coordination sphere onwards.

The definition of the radial distribution function may be extended to apply to a mixture of different atoms, but even the binary system requires a lot of extra experimental data for a complete one-dimensional (radial) description of the structure. Three different measurements with different radiations, or on mixtures with different chemical or isotopic composition are needed to define the partial distributions  $\rho_{AA}(r)$ ,  $\rho_{BB}(r)$  and  $\rho_{AB}(r)$ . In such systems a new method which derives the radial distribution function around an atom from the fine structure near its X-ray absorption edge may prove useful [18]. Some directional information about amorphous structures is also beginning to emerge from improved electron diffraction techniques.

Structural analysis is performed by comparing the measured radial distribution function with that predicted on the basis of some model. The models can be roughly categorised according to the degree of short-range order. The *frozen gas* model allows very little. The *continuous random network* models, appropriate for covalently bonded solids where the bonds have strong directional quality, and the *random dense packing* models for metallic solids preserve a high degree of order in the first one or two coordination spheres. In *microcrystalline* models the short range order extends over distances of 10-15 Å, permitting a reciprocal lattice to be defined.

Continuous random network models seem to be most appropriate for describing materials such as amorphous germanium, silica, or  $\text{As}_2\text{Se}_3$  [19]. The models are literally built with ball and stick units [20] or space filling polyhedra [21] which represent the basic

structural block, an  $\text{SiO}_4$  tetrahedron for example, but they are assembled in such a way as to allow random variations in the bond lengths and inter-bond angles. Otherwise the models may be constructed in the computer subject to some steric restraints such as three-coordination for arsenic and two coordination for selenium in  $\text{As}_2\text{Se}_3$ , derived from the  $8 - N$  rule for covalent bonding ( $N$  is the number of valence electrons). Computer routines can also minimise the free energy by simulating thermal motions and allowing the bonds to relax or the structure to adjust to fill voids. Such continuous random networks are capable of reproducing the observed radial distribution function, whereas microcrystallite models fail to reproduce its detailed structure despite considerable ingenuity in modifying the crystallites by defects, setting them in an amorphous matrix or mixing known or unknown structural polymorphs [22].

A random network model is also widely accepted for the silicate glasses, the network being formed of Si-O chains which intersect at every Si node so giving the  $\text{SiO}_4$  tetrahedra. The silicon, or anything that will take its place in a *glass former*. Other elements, which occupy interstitial sites in the network, are *modifiers*. The chalcogenides selenium and tellurium preserve large molecular units in the amorphous state, as do polymers. The units are more or less randomly ordered with respect to each other, and may be cross-linked by adding other elements.

The structures of amorphous alloys differ from those of amorphous semiconductors in that their coordination number is much greater,  $\sim 8-12$ . The Bernal model [23] of densely packed spheres is capable of accounting for the radial distribution functions of several metallic alloys, and notably for the splitting of its second peak which is not consistent with microcrystallites [24].

Amorphous structures still remain largely unknown. Only a handful of them have been modelled yet, and theoretical attention has been focussed on the simplest, monatomic ones. The amorphous materials of practical interest usually contain two components at the very least, and detailed information about the structure of such materials is completely lacking. In such a simple and widely studied a material as GeTe, even the coordination numbers of Ge and Te are uncertain, though they are known to differ from those of the crystalline phase. In these circumstances, any scraps of structural information are welcome.

1.4 PHYSICAL PROPERTIES AND APPLICATIONS. — A change in the coordination number and bonding is likely to result in important differences in the physical properties of amorphous and crystalline phases of the same material. Frequently, however, these parameters are do not change, and differences in electronic structure are found nonetheless. For instance, crystalline tellurium is a metal, amorphous tellurium a semiconductor.

The principal effects of a potential varying randomly in space on the electronic structure (formally equivalent to a periodic potential of randomly varying amplitude) are to smear out the sharp band edges into band tails, and to localise the electronic states in these tails. The transport properties of an amorphous semiconductor are dominated not by the band gap, but by the larger mobility gap [1]. The optical absorption spectra of amorphous materials tend to exhibit less fine structure, and a shifted absorption edge relative to the crystalline forms [25].

A host of devices for switching, photography and data storage are based on the differences in physical properties of crystalline and amorphous materials, and on the possibility of inducing crystalline  $\leftrightarrow$  amorphous transitions by application of light or electrical pulses [26]. As an example of such applications we mention the memory switch [27]. The resistivity of thin films of a glass such as  $\text{Te}_{81}\text{Ge}_{15}\text{As}_4$  drops abruptly when a certain voltage threshold is exceeded. The low resistance state is stable unless the device is reset using a large current pulse. These devices can obviously be used to store binary information. The explanation of the behaviour is thought to be the formation of filaments of crystalline, metallic tellurium at the threshold voltage. The reset pulse heats the whole film momentarily above  $T_g$ , and serves to revitrify it.

Other devices based on amorphous materials range from electrochromic displays [28] to magnetic bubble domain memories [29]. The magnetic properties are discussed in § 3.1.

**1.5 USE OF MÖSSBAUER SPECTROSCOPY.** — The Mössbauer effect provides essentially local information; the electric and magnetic fields at a nuclear site, the mean square velocity and displacement of the resonating nucleus. The isomer shift and quadrupole interaction are determined mainly by the immediate neighbours, so it should be possible to learn something of the bonding, coordination number and local structure around the Mössbauer atom.

Unfortunately the best glass formers, a cluster of elements around arsenic in the periodic table, are not the best candidates for Mössbauer studies. Si, As and Se have no suitable resonance and Ge, with two, presents formidable technical difficulties. To observe the 67 keV resonance one must resort to Cr [30], whereas the 13 keV resonance [31] may suffer (like NMR) from too high a resolution for investigating amorphous solids! Sb and Te possess more tractable Mössbauer isotopes, and some useful information has been obtained on tellurium and antimony-based glasses. Fe and Sn can be incorporated into oxide or chalcogenide glasses as a minor constituent, though neither is a very good glass former. However amorphous compounds and alloys of iron do exist, and the Mössbauer effect is particularly suitable for studying their magnetic properties. The rare earths, Eu and Tm have also been studied in oxide glasses. Radio-

isotopes, notably  $^{129\text{m}}\text{Te}$  have been used for source experiments.

Besides the information obtainable about the structure, bonding and magnetic properties from the hyperfine interaction parameters, the scattering of Mössbauer radiation is a potentially valuable way of studying both the structure and atomic displacements of materials which do *not* contain Mössbauer atoms. The work along these lines is fully discussed in the following paragraphs. More details of work on the glass transition itself, based on a sharp fall of the recoilless fraction  $f$  in the supercooled liquid may be found in references [7].

**2. Structure and bonding.** — **2.1 MÖSSBAUER SCATTERING.** — In scattering experiments [32] the Mössbauer source provides a flux of extremely monochromatic radiation, comparable in wavelength to X-rays. The elastically scattered fraction  $f'$  and the linewidth of the scattered radiation are then measured

$$f' = \gamma \exp(- (2 \pi s)^2 / \langle x^2 \rangle). \quad (2)$$

Here  $\gamma$  is the ratio of Rayleigh to Rayleigh and Compton scattering, and  $\langle x^2 \rangle$  is the mean square atomic displacement.  $f$  is obtained by measuring the count rates with a black absorber between source and sample or source and counter, both on and off resonance. The temperature variation of  $f'$  has been related to ideas of atomic motion in the glassy, supercooled liquid and liquid phases of several organic compounds by Champeny and Sedgwick [33], and one of their results is shown in figure 3.  $\ln f'$  is linear in  $T$  in the glass,

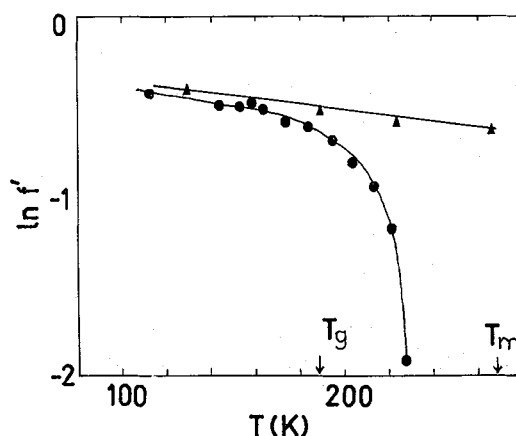


FIG. 3. — Temperature-dependence of the elastic scattering of Mössbauer radiation from diethyl phthalate in the glassy (●) and crystalline (▲) forms. The glass and melting transitions are marked (from ref. [33]).

though smaller than in the crystal. Above  $T_g$  it begins to fall precipitously, and it becomes unmeasurably small near  $T_m$ . The large value of  $\langle x^2 \rangle$  above  $T_g$  ( $\sim 2 \text{ \AA}^2$ ) was explained by librational oscillations of the molecules, which give way to free rotations near  $T_m$ . Line broadening observed near  $T_m$  was ascribed to a diffusion process.

Variations of the recoilless fraction,  $f$ , have also been observed near  $T_g$  in conventional absorber experiments [34].

A measurement of the elastic scattering as a function of  $s$  can be used, in principal, to derive a radial distribution function of the equilibrium atomic positions, which is different from that obtained in the normal X-ray scattering experiments, where inelastic scattering is also counted. Albanese and Ghezzi [35] have succeeded in separating the elastic and inelastic scattering from amorphous  $\text{SiO}_2$  using the Mössbauer effect, which is still unsurpassed by any other technique in its energy resolution. Their results are shown in figure 4. Regret-

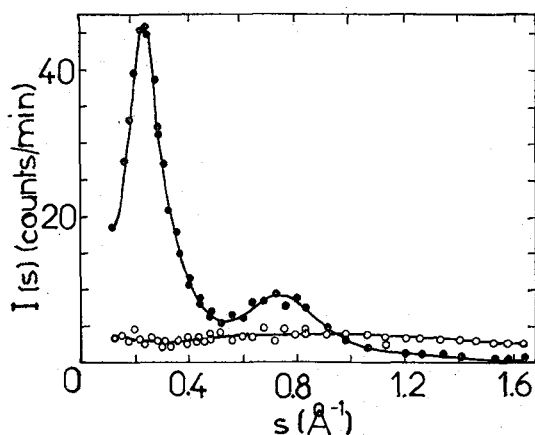


FIG. 4. — Scattering vector dependence of the elastic (●) and inelastic (○) scattering of Mössbauer radiation from vitreous silica at room temperature (from ref. [35]).

tably, poor statistics and experimental uncertainties prevented them from deriving the radial distribution function from the elastic scattering. The inelastic scattering, corrected for Compton scattering gave the thermal diffuse scattering which was found to depend on  $T$  and  $s$  in the way expected for an Einstein solid.

Useful structural information may be obtainable by Mössbauer scattering if the quality of the data can be improved by using the multicounter techniques common in neutron scattering.

2.2 OXIDE GLASSES. — 2.2.1  $^{57}\text{Fe}$ . — Well over one hundred silicate, phosphate, borate and more complex mixed oxide glasses containing iron have been examined by Mössbauer spectroscopy since the first work by Pollak *et al.* [36] demonstrated that it was possible to observe the effect in a noncrystalline material. The structural aspects are discussed here, the magnetic properties being deferred to § 3.2.1. The earlier results are fully expounded in Kurkijan's 1970 review [6], so we treat the subject briefly.

It is generally admitted that iron ions in these glasses are surrounded by oxygens, so the main structural information available from Mössbauer studies is the iron coordination number and valence. The coordination number in a silicate glass for instance tells whether

the iron is a glass former (four-coordinated, replacing silicon) or a network modifier (six-coordinated, in an interstitial position). This information has helped in understanding the chemical processes involved in slags [37] or in glass-steel bonds [38].

The isomer shift  $\delta$  is plotted against quadrupole splitting  $\Delta$  for numerous oxide glasses in figure 5. The

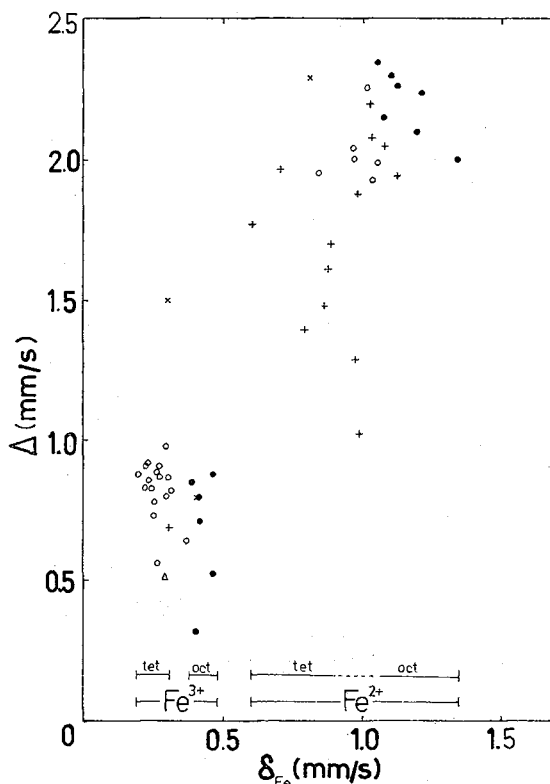


FIG. 5. — Compendium of isomer shifts and quadrupole splittings for iron in a variety of oxide glasses ○ Alkali silicates; × Alkaline earth silicates; △ Alkali borates; ● phosphates; + others.

data is taken from many sources, and is of variable quality. Often iron is found in two valence states, or in different coordinations in the same glass, and careful analysis is needed to separate the subspectra. A typical spectrum is shown in figure 6. For  $\text{Fe}^{3+}$  in the alkali silicate [37, 38, 40-45] and borate [46] glasses, the isomer shifts all fall in the range 0.19-0.31 mm/s (relative to iron metal) which coincides with the range of isomer shifts of the tetrahedrally coordinated ferric ion in crystalline oxides and silicates. The  $\text{Fe}^{3+}$  isomer shift data for phosphate glasses [40, 45, 48, 49] all falls in a separate narrow range, 0.37-0.47 mm/s, which corresponds to octahedral coordination. In alkaline earth silicate glasses, ferric iron is found in both coordinations [37, 39, 50], whereas in alkaline earth borates its coordination is octahedral [129].

The coordination of  $\text{Fe}^{2+}$  is not so clear-cut. Although it is highly probable that an isomer shift less than 0.9 mm/s indicates tetrahedral coordination, and

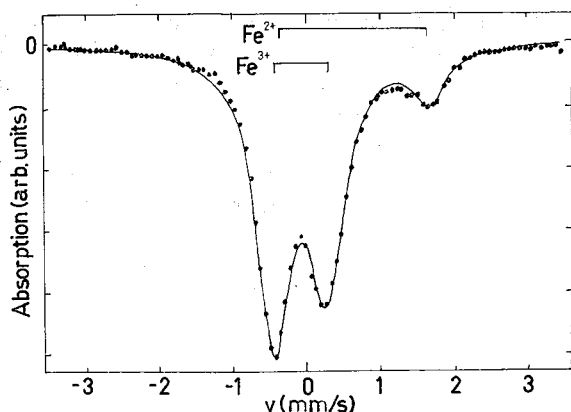


Fig. 6. — Typical Mössbauer spectrum of  $^{57}\text{Fe}$  in an alkali silicate glass ( $67\text{SiO}_2$ ,  $18\text{K}_2\text{O}$ ,  $15\text{Fe}_2\text{O}_3$ ) (from ref. [39]).

one greater than 1.05 mm/s octahedral coordination, there is a region around 1 mm/s where the two ranges may overlap. The greater isomer shift for octahedrally coordinated iron reflects the greater ionicity of the bond. Previous suggestions of a correlation between coordination number and quadrupole splitting [47] appear to be unfounded, though there might be a tendency for a greater ferrous splitting in octahedral than in tetrahedral coordination.

In the alkali silicate glasses there seems to be a tendency for the ferrous coordination to change from four to six with increasing iron concentration ( $\geq 3$  mole %). Furthermore, at the low iron concentrations the  $\text{Fe}^{2+}/\text{Fe}^{3+}$  ratio measured from the Mössbauer spectrum increases sharply, though the same effect is not found by chemical analysis [41, 42, 44, 47]. This discrepancy has not been explained, but a qualitative explanation for the relative increase in  $\text{Fe}^{2+}$  has been suggested [44]. A difference in the recoilless fractions for  $\text{Fe}^{2+}$  and  $\text{Fe}^{3+}$  in octahedral sites in an aluminophosphate glass has been detected [49], but it is much too small to explain the effect.

The line broadening found for both ferric and ferrous ions in these glasses has been variously explained. The linewidth is typically two or three times the natural linewidth, and many authors have attributed this to a distribution of electric field gradients in the amorphous material. Broadening of the  $\text{Fe}^{3+}$  lines in glasses with low overall iron concentrations can be due to incipient paramagnetic hyperfine structure [53], but diffusion effects might also be present [44]. Another possible explanation would be rapid  $\text{Fe}^{2+} \leftrightarrow \text{Fe}^{3+}$  electron transfer, which has been shown to be present in a study of the electrical properties of a lead silicate glass containing iron [54]. The polaron hopping frequency is of order  $10^{-5}$  s, close to the value necessary to give appreciable broadening of resolved ferrous and ferric spectra. A Mössbauer study of such charge transfer should be feasible, and in any case a systematic study of the origins of the line broadening would be useful.

The chemical state of iron in the oxide glasses depends sensitively on the preparation conditions

(oxidising or reducing atmosphere) and heat treatment. Under certain circumstances, and particularly when the iron content exceeds about ten mole percent, there is a tendency for finely divided iron oxides or ferrites to segregate [43]. In all impurity studies care has to be taken to ensure that the observed spectrum is really related to the glass, and not to some precipitated phase.

2.2.2  $^{119}\text{Sn}$ . — Tin has been studied as a component of alkali silicate [55-58] borate [57] and more complex oxide glasses [59, 60] by a number of Russian workers, and information has been obtained, similar to that for iron, about the valence, coordination number and bonding.

In the alkali silicates for which  $\text{SnO}_2$  has been included in the melt, the tin is entirely quadrivalent with an isomer shift and quadrupole splitting both slightly different from  $\text{SnO}_2$ . A coordination number of six is inferred from the similarity of the temperature-dependence of the recoilless fraction to that of the oxide [57]. The isomer shift depends more on the alkali cation, decreasing in the sequence Li-Na-K, than on the composition of the glass, and the rigidity of the bond, determined from  $f(T)$ , decreases in the same sequence. The increase in ionicity of the Sn-O bond with increasing radius of the alkali cation is confirmed by position annihilation [58]. Mitrofanov and Siderov suggest that not only are the six oxygens of the first coordination sphere retained in the glass, but also the second sphere (silicon and alkali cations) has a constant configuration so that well defined structural blocks exist around the tin. Divalent and quadrivalent tin are found in the alkali silicate glasses when tin metal is included in the melt, and the same is also true of a glass made simply from  $\text{SnO}_2$  and  $\text{SiO}_2$  [57] and of a soda lime silica window glass made with tin metal [60]. In the latter case, the  $\text{Sn}^{\text{IV}}/\text{Sn}^{\text{II}}$  ratio increased after dealkalization of the surface, a commercial process for strengthening plate glass.

The Mössbauer spectrum of tin in glass fibres made from some multi-component silicate glasses was found to be narrower and asymmetric compared to that of the bulk glass (Fig. 7). The phenomenon was attributed to the tin acting as a glass former, despite its six-coordination. In the drawn fibre it was inferred that there was some structural orientation, and a narrower distribution of electric field gradients. Heat treatment of the fibres destroyed the structural orientation and give back the bulk spectrum. The spectrum of other glasses, with different compositions, was no different for fibres or bulk. Tin in these glasses thus may sometimes play the role of glass former, and sometimes that of network modifier [59].

2.2.3 Other isotopes. — The rare earths Tm [61] and Eu [62] have been studied as impurities in oxide glasses. In both cases the spectra are similar to those of the sesquioxides, indicating that the rare earths are trivalent and occupy well defined octahedral sites. An analysis of the temperature dependence of the quadru-

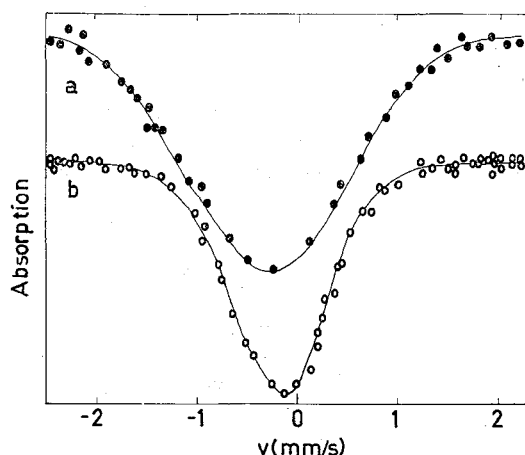


FIG. 7. — Mössbauer spectra  $^{119}\text{Sn}$  in *a*) a glass with composition (65  $\text{SiO}_2$ , 20  $\text{Na}_2\text{O}$ , 8.5  $\text{CaO}$ , 6.5  $\text{SnO}$ ) *b*) oriented fibres of the same glass. The zero of velocity corresponds to the position of the peak for crystalline  $\text{SnO}_2$  (from ref. [59]).

pole splitting for Tm was hampered by a lack of knowledge of the exact local symmetry, but there was a strong suggestion that the thulium valence electrons participate in covalent bonding. Broadening of the europium line in silicate and phosphate glasses was attributed to unresolved quadrupole splitting and disorder in the glass structure. The recoilless fraction was a little smaller in the glass than in the oxide, both at 300 K and at 4.2 K.

The  $^{121}\text{Sb}$  resonance has been studied in phosphate glasses made with  $\text{Sb}_2\text{O}_3$  and another transition metal oxide. The antimony is trivalent for all cases except for vanadium where some quinivalent antimony is found [63].

**2.3 CHALCOGENIDE GLASSES.** — **2.3.1 Tellurium-based glasses.** — With the possible exception of tin, tellurium is the only element which has been examined in the amorphous state by Mössbauer spectroscopy [64]. Amorphous, pure tellurium cannot be obtained by quenching the melt, so the measurements of Blume were made on evaporated  $2\ \mu$  films.  $f$  was found to be three times smaller in the amorphous phase at 4.2 K than in the crystalline phase, and the quadrupole splitting was slightly increased. The latter change may be due to a shortening of the Te-Te bonds in the spiral tellurium chains which are the basic molecular unit in both phases, since Boolchand *et al.* have found a correlation between  $\Delta$  and Te-X bond length in isostructural compounds [65]. Most interesting, however was the large anisotropy of the quadrupole doublet which need not be interpreted as showing that the amorphous phase has an oriented microcrystalline structure. An amorphous structure with preferred orientation of the tellurium chains could produce it. Even a continuous random network model of germanium and ice has been found to possess marked anisotropy [66].

Boolchand and co-workers have made a rather extensive study of spluttered  $\text{Ge}_x\text{Te}_{1-x}$  films as a function of composition, temperature and heat treatment [67]. One of their results is an extrapolated value  $\Delta = 9.60\ \text{mm/s}$  for  $x = 0$ , corresponding to a Te-Te bond length of  $2.62\ \text{\AA}$ , but it is uncertain that the structures of amorphous pure and germanium-doped tellurium are similar. For small values of  $x$ , the values of  $\Delta$  and Te-Te bond length (derived from the radial distribution function) were found to be consistent with the systematic of the Te-X bond length in crystalline compounds. The spectra of the recrystallised films differed considerably from the amorphous ones. The example of GeTe is shown in figure 8. The crystalline

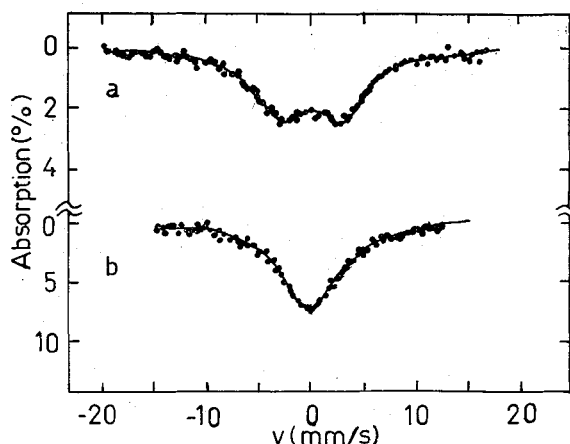


FIG. 8. —  $^{125}\text{Te}$  Mössbauer spectra of  $120\ \mu$  GeTe films taken at 78 K *a*) is amorphous, *b*) is crystalline (from ref. [67]).

form has a slightly distorted NaCl structure (6 : 6 coordination) and a very small unresolved quadrupole splitting, whereas the amorphous spectrum is quite different and might be consistent with either the 4 : 2 or 3 : 3 coordinations which have been proposed [68]. The effect of annealing a GeTe<sub>2</sub> film is to reduce  $\Gamma$ , increase  $\Delta$  and double  $f$ , which all suggests a greater degree of order in the local environment due to the relaxation of bonds. Two other amorphous tellurium alloys have been studied directly. One,  $\text{Te}_{70}\text{Cu}_{25}\text{Au}_5$  gave a spectrum similar to that of crystalline tellurium, which is expected if the alloy contains short, randomly oriented tellurium chains, similar to those forming the basis of the Te structure [69]. The other,  $\text{Te}_{81}\text{Ge}_{15}\text{As}_4$  is a memory switching glass. A lower quadrupole splitting was found in the crystalline than in the amorphous state, but the difference was much more evident when the glass was prepared with radioactive  $^{129m}\text{Te}$ , and the  $^{129}\text{I}$  resonance was observed. It was suggested that the method might be used to detect crystalline filaments in the switched material [70].

Despite recent advances in source preparation [67] the  $^{125}\text{Te}$  studies are handicapped by the poor resolution of the resonance. The quadrupole splittings are at most comparable to the linewidth and the isomer shifts are even smaller, so that the spectra should best be



fitted using the transmission integral approach [71]. Nevertheless the Mössbauer spectra have given some useful corroborations of the chain model for the tellurium-rich compositions by showing that the site symmetry and bonding resemble those in the metal. Some of the  $^{125}\text{Te}$  data is summarised in Table I.

2.3.2 *Selenium-based glasses.* — There are several structural modifications of crystalline selenium. The trigonal form is isomorphous with tellurium with the same spiral chains, bound together by van der Waal's forces. The monoclinic forms are both built of puckered  $\text{Se}_8$  rings. Amorphous selenium has been studied by doping it with  $^{125}\text{Te}$  [72, 73] and  $^{119}\text{Sn}$  [74].

The tellurium spectra for the two crystalline modifications show slightly different quadrupole splittings [72] and the amorphous form gives a splitting intermediate between the two [72, 73]. This is interpreted as showing that both structural units are present in the amorphous phase, and the proportion of rings and chains could be derived from the spectrum of samples quenched from different temperatures, if the probability of tellurium substituting in either unit were known.

The temperature dependence of  $f$  for tin impurities in crystalline, amorphous and microcrystalline (80–100 Å) selenium has been measured and fitted to the low frequency part of the phonon spectrum using neutron scattering data and the Debye model.  $f$  was greatest in the crystalline and least in the microcrystalline samples [74].

Selenium-based glasses containing Ge and Sn showed only  $\text{Sn}^{\text{IV}}$  in the glass-forming region with a spectrum resembling that of  $\text{SnSe}_2$ . It was suggested that tin in the glass was bound in structural units intermediate between six- and four-selenium coordination [75]. In the quaternary system Se-As-Ge-Sn, both  $\text{Sn}^{\text{IV}}$  and  $\text{Sn}^{\text{II}}$  were found in the glass-forming region. The  $\text{Sn}^{\text{II}}$  was also bound to selenium [76]. The Se-As-Sn system is discussed below.

2.3.3 *V-VI glasses.* — The semiconducting  $\text{V}_2\text{VI}_3$  glasses are of considerable interest because of an

optically induced shift in their absorption edge which can be reversed by annealing near  $T_g$ . Some IV-V-VI glasses show threshold or memory switching. The amorphous materials are believed to be constructed of molecular units in which the 8- $N$  rule is respected. In  $\text{As}_2\text{Se}_3$ , for example, the As has three neighbours and the Se has two neighbours [77].

A Mössbauer study of the complete ternary field Se-As-Sn has been reported [78] and other authors have studied compositions in and near the glass-forming region [79–82]. For low tin concentrations ( $\leq 5\%$ ) the spectrum is a well defined doublet with parameters close to those for  $\text{SnSe}_2$ . In  $\text{SnSe}_2$ , the tin is bound to six selenium neighbours. Some authors have suggested that the smaller and more temperature-dependent recoilless fraction in the glass compared with  $\text{SnSe}_2$  indicates that the tin is four-coordinated by selenium [79], as might be expected from the valence, but the inference is not clear-cut and seems to be made as much from chemical considerations as from the Mössbauer data. The small difference in isomer shift compared with  $\text{SnSe}_2$  is ascribed to the influence of the seleniums' other neighbours. At higher tin concentrations a spectrum resembling  $\text{SnSe}$  begins to emerge, but the details of the  $\text{Sn}^{\text{IV}}/\text{Sn}^{\text{II}}$  ratio depend on the preparation method and there is disagreement whether the divalent tin appears within [81] or beyond [80] the limits of the vitreous phase. Although tin is quadrivalent in amorphous  $\text{As}_2\text{Se}_3$ , it is divalent in the crystal where the coordination number is probably three. Electrically, the crystal-glass transition is marked by the disappearance of impurity conduction, and this may be explained by the change of tin valence and saturation of all its bonds in the glass [82].

The glasses  $\text{As}_2\text{Te}_3$  and  $\text{As}_2\text{Se}_3\text{-As}_2\text{Te}_3$  have been studied as absorbers containing  $^{119}\text{Sn}$  and as sources containing  $^{129\text{m}}\text{Te}$ . Tin spectra in crystalline and vitreous  $\text{As}_2\text{Se}_3\text{-As}_2\text{Te}_3$  are like that of  $\text{SnSe}_2$  but in  $\text{As}_2\text{Te}_3$  there are substantial differences. The spectra were analysed as containing three components associated with tin with only arsenic, only tellurium

TABLE I

 $^{125}\text{Te}$  Data for Amorphous and Crystalline Tellurium Compounds

	$T$ (K)	Amorphous		Crystalline		References
		$\delta$ (*) (mm/s)	$\Delta$ (mm/s)	$\delta$ (*) (mm/s)	$\Delta$ (mm/s)	
Te	4.2	(0.41)	(9.60)	0.50	7.74	[67]
		(extrapolated from $\text{Ge}_x\text{Te}_{1-x}$ )				
	78			—	7.3	[69]
$\text{Te}_{70}\text{Cu}_{25}\text{Au}_5$	78	—	7.4	—	—	[69]
$\text{Te}_{81}\text{Ge}_{15}\text{As}_4$	78	0.60	8.7	0.86	6.1	[70]
GeTe	4.2	0.22	6.17	—	—	[67]
$\text{GeTe}_2$	4.2	0.27	7.80	—	—	[67]

(\*) Relative to a  $^{125}\text{SbCu}$  source.

or a mixture of neighbours [83]. The difference between crystalline and amorphous  $\text{As}_2\text{Te}_3$  was particularly marked in the source experiment (Fig. 9), and the large quadrupole splitting in the amorphous phase was associated with a layer structure (found in both amorphous and crystalline  $\text{As}_2\text{Se}_3$ - $\text{As}_2\text{Te}_3$ ) whereas the crystalline structure is almost cubic [84].

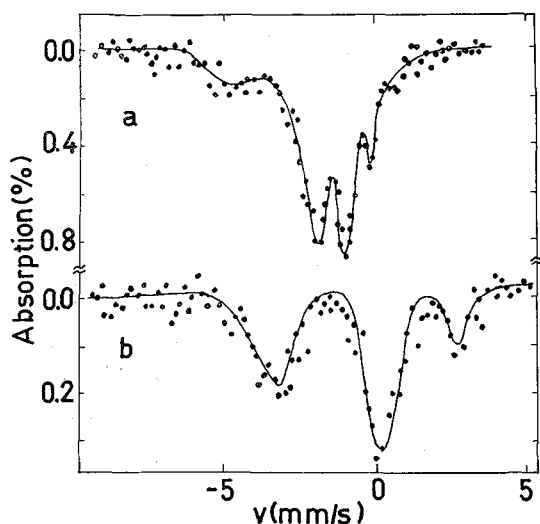


FIG. 9. — Mössbauer spectra of a) crystalline and b) amorphous  $\text{As}_2\text{Te}_3$  doped with  $^{129\text{m}}\text{Te}$ . The absorber was  $\text{K}^{129}\text{I}$  (from ref. [84]).

Amorphous and crystalline  $\text{Sb}_2\text{X}_3$ ,  $\text{X} = \text{O}, \text{S}, \text{Se}$ , have been studied directly using the antimony resonance [85-87] and the Mössbauer parameters are summarised in Table II. In the two crystalline forms of  $\text{Sb}_2\text{O}_3$  the antimony is bonded to three oxygens at a distance of 2.0 Å with a similar geometrical configuration. The near identity of the parameters suggests that the same coordination and bonding of the antimony is retained in the amorphous phase [85]. In the crystalline selenide there are two equally populated antimony sites with different isomer shifts and quadrupole interactions, yet the amorphous spectrum shows only a single, narrow range of antimony environments. The data excludes the possibility that the amorphous structure might be microcrystalline. Furthermore, there were

only small differences in line width and quadrupole interaction over a wide range of composition  $\text{SbSe}_x$ ,  $6.3 > x > 0.5$ , suggesting that the antimony bonds to three seleniums throughout the composition range [87]. The increase of isomer shift in amorphous  $\text{Sb}_2\text{X}_3$ , in the order O, S, Se corresponds to an increase in s-electron density at the nucleus. As it is mainly p-bonding in these compounds, the changes in  $\delta$  are consequently rather small.

2.4 OTHER AMORPHOUS MATERIALS. — So far there have been few studies of amorphous metals and alloys and those that there are have been mostly concerned with their magnetic properties (§ 3.3).

200 Å tin films spluttered onto a cold substrate are superconducting at 4.2 K whereas annealed  $\beta\text{Sn}$  films are not. The spluttered films are probably amorphous, and give an isomer shift 0.2 mm/s greater than for the crystalline films [88].

The Mössbauer effect has claimed to have been observed for  $^{119}\text{Sn}$  in liquid gallium globules ( $\sim 70$  Å) dispersed in a porous glass matrix [89].

Some work on  $\text{Fe}_x\text{Ge}_{1-x}$  in progress in our laboratory has shown that the system becomes metallic and orders magnetically when a critical concentration  $x \sim 0.25$  is exceeded. This is close to the percolation limit of the iron, if iron and germanium were randomly packed [90]. The Mössbauer spectrum of the 5 000 Å  $\text{FeGe}$  film shown in figure 1 has an isomer shift of 0.45 mm/s relative to iron metal, close to that of the cubic phase of ordered, crystalline  $\text{FeGe}$ .

Amorphous iron-bearing minerals have not been widely studied, except for glasses of lunar [91] and meteoric origin [92]. Also a natural amorphous ferric gel has been characterised by its Mössbauer spectrum [93] and identified as a major component of lake sediments [94]. Synthetic gels have been studied by a combination of Mössbauer and other techniques, and have variously been reported as being amorphous [95] or microcrystalline [96], but the structure is strongly dependent on the preparation technique. The amorphous/microcrystalline question cannot be resolved from the Mössbauer spectra of these compounds, although an estimate of the particle size may be obtained from the superparamagnetic behaviour [93,

TABLE II

$^{121}\text{Sb}$  Data for Amorphous and Crystalline Antimony Chalcogenides (ref. [85-87])

	$\delta$ (*) (mm/s)	Amorphous $e_2 qQ$ (mm/s)	$\delta$ (*) (mm/s)	Crystalline $e^2 qQ$ (mm/s)
$\text{Sb}_2\text{O}_3$	- 11.3	18.3	- 11.3	18.3 (Cubic)
			- 11.3	17.0 (Orthorhombic)
$\text{Sb}_2\text{S}_3$	- 12.7		- 14.3	—
$\text{Sb}_2\text{Se}_3$	- 13.6	10.9	- 12.6	7.9
			- 15.5	8.4 (2 sites)

(\*) Relative to a  $\text{SnO}_2$  source.

96]. The vitrification of clay minerals on firing is a central concern of ceramicists and some Mössbauer studies have been reported [97, 98] including the use of the Mössbauer effect to help determine the firing temperature of ancient pottery [99]. Some more systematic work in this area could be of great practical interest.

### 3. Magnetic properties. — 3.1 INTRODUCTION. —

Magnetic exchange interactions depend strongly on the distance between interacting atoms, and on bond angle for superexchange. They also depend on the number of interacting neighbours. On equivalent sites in crystalline materials these parameters have a fixed value. Amorphous materials have no equivalent sites, and the distance, angle and number take a multitude of values. The essential difference between crystalline and amorphous magnets is that the constant exchange interaction at any site is replaced by a spatial distribution of exchange interactions.

*Ferromagnetism* is conceptually the simplest type of magnetic order which can exist in an amorphous solid (Fig. 10a). It was first suggested theoretically by

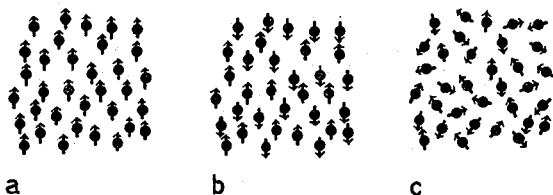


FIG. 10. — Three types of magnetic order which may be found in amorphous solids a) ferromagnetism b) antiferromagnetism c) spermagnetism.

Gubanov [100], and subsequently observed in a number of metallic alloys [101]. The molecular field model for crystalline ferromagnets may be extended to amorphous ones by replacing the molecular field  $H_m$  by a distribution of fields so that  $P(H_m)$  is the probability of an atom being subject to a certain field.

Handrich [102] characterises a narrow  $P(H_m)$  distribution by its width defined by

$$\Delta'^2 = \langle (H_n - \bar{H}_n)^2 \rangle / \langle H_m \rangle^2$$

where  $H_n$  is the average value of  $H_n$  and obtains

$$\langle \sigma \rangle = \frac{1}{2} \{ \mathcal{B}_S[x(1 + \Delta')] + \mathcal{B}_S[x(1 - \Delta')] \} \quad (3)$$

where  $\langle \sigma \rangle$  is the average reduced magnetisation of an atom,  $\mathcal{B}_S$  is the Brillouin function for spin  $S$  and  $x$  is its usual argument  $3S\sigma/(S+1)\tau$  where  $\tau$  is the reduced temperature. Eq. (3) predicts a flatter reduced magnetisation curve the greater the value of  $\Delta'$ . There is no ferromagnetic state if  $\Delta'$  exceeds 1. If only nearest-neighbour distances varied randomly in the amorphous phase, a narrow  $P(H_m)$  distribution is physically reasonable. However if the number of interacting neighbours is also variable and the exchange

is short-ranged a distribution with peaks corresponding to different numbers of atoms in the first coordination sphere must be used (Fig. 11c).

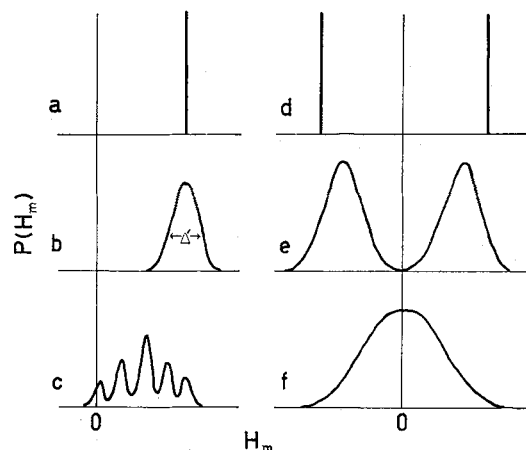


FIG. 11. — Schematic molecular field probability distributions a) for the crystalline ferromagnet, b) for the amorphous ferromagnet with a distribution of nearest neighbour distances, c) for the amorphous ferromagnet with a distribution of nearest neighbour distances and number of interacting neighbours, d) for the crystalline antiferromagnet e) for the amorphous antiferromagnet with an open structure and f) for the amorphous antiferromagnet with a closed structure (adapted from ref. [102-105]).

Amorphous *antiferromagnetism* is not so evident, either theoretically or experimentally although it is easy enough to picture two inter-penetrating sublattices and a symmetric distribution of molecular fields as shown in figures 10b and 11e. The molecular field model has been developed by several authors [103, 104] and the problem has been discussed by Simpson in an article entitled « Does the amorphous antiferromagnet order ? » [105]. He distinguishes between open structures (like the bcc crystal structure) where the nearest neighbours of a given magnetic atom do not interact strongly among themselves and where the bimodal  $P(H_m)$  may be appropriate, and closed structures (like the fcc crystal structure) where neighbours do interact strongly. In the amorphous analogues of the latter, which might include *all* amorphous materials with antiferromagnetic interactions, the most probable exchange field is zero, and the Néel temperature is at least likely to be greatly reduced in the amorphous state. A consequence of the overall lack of magnetocrystalline anisotropy is that there should be no spin wave gap as in the crystalline antiferromagnet, and large localised spin waves may be expected in regions of low exchange energy, even at  $T = 0$ . Tahir-Khelli [106] has used a more sophisticated theoretical approach to show that misfit between sublattices (wrong bond configurations) reduces the Néel temperature, and at a critical value the antiferromagnetic state breaks down as the zero-point spin deviation becomes equal to the spin magnitude. These

considerations suggest that amorphous antiferromagnetic order is most likely to be found in systems containing ions with large spins, such as  $\text{Fe}^{3+}$  or  $\text{Mn}^{2+}$ , although an antiferromagnetic exchange interaction is not precluded for other ions. Some confirmation of this idea may be provided by measurements on a series of transition metal phosphate glasses [107].

Amorphous *ferrimagnetism* has been postulated to explain the small saturation moment found in  $\text{Ni}_{85}\text{P}_{15}$ . This would require very broad, asymmetric  $P(H_m)$  distribution giving some reversed spins [108]. Such a structure could be nicely tested by Mössbauer spectroscopy in an applied field.

All the ordered structures just mentioned possess a preferred axis, although the amorphous material frequently does not. In crystalline materials, magnetic structures in which the direction of the ordered moment varies from site to site are well known; the helimagnetic structures in rare earth metals or the Yafet-Kittel arrangements in certain ferrites for example. A counterpart in amorphous materials is *speromagnetism* defined as an order having short range correlations of spin directions but no average long range correlations [109]. The correlations of the spin directions thus somewhat analogous to those of the atomic positions. *Order* in this context is to be understood in the sense that an amorphous solid is ordered, but a liquid or a paramagnet is not. In other words, the time average of the correlation between any two atomic spins  $\overline{S_i \cdot S_j}$  is not zero. The spin structure is indicated schematically in figure 10c and the author has used the Mössbauer effect to show that speromagnetism exists in at least one amorphous material [109] (§ 3.2.3).

Finally, a theoretical model for amorphous magnetism has recently been suggested by Harris *et al.* [110]. It is based on the Hamiltonian

$$\mathcal{H}_i = V_i - \frac{1}{2} J \sum_{\delta'} S_i S_{i+\delta'},$$

where  $V_i$  is a very strong randomly varying single-ion anisotropy due to the local site distortions at a site  $i$ ,  $J$  is the exchange interaction, and  $\delta'$  are the nearest neighbours. This model is appropriate for rare-earth alloys, where the two terms in the Hamiltonian are of comparable magnitude. In the case of uniaxial anisotropy and ferromagnetic exchange the spin directions could make angles of up to  $90^\circ$  with the ferromagnetic axis. This structure might perhaps be regarded as a special case of speromagnetism, where the spins make angles up to  $180^\circ$  with any arbitrary axis.

Mössbauer work on noncrystalline magnets is reviewed in the following paragraphs. Unlike the structural studies, it is not voluminous and is all concerned with the iron resonance. A short discussion of work on random solid solutions is included because it is possible to examine one aspect of magnetic amorphousness in isolation in these systems, namely the variation in the number of magnetic neighbours. The exchange is essentially short-ranged, and the bond lengths and angles fixed. The discussion stops

short of disordered or dilute alloys where the longer range of the interaction spoils the simplicity of the problem.

A short, general review of topics in amorphous magnetism has been given by Hooper [111].

3.2 NONMETALS. — 3.2.1 *Iron in glasses.* — The magnetic properties of iron in oxide glasses have been the object of several studies [6, 43, 46, 53, 108], the most extensive being that of Bukrey *et al.* [46] on alkali borate glasses. Alkali silicate [43, 53, 108] and phosphate glasses [53] have been less extensively studied.

Following Bukrey *et al.*, some of whose data is shown in figure 12, the magnetic properties of iron in oxide glasses may be summarized as follows. Below

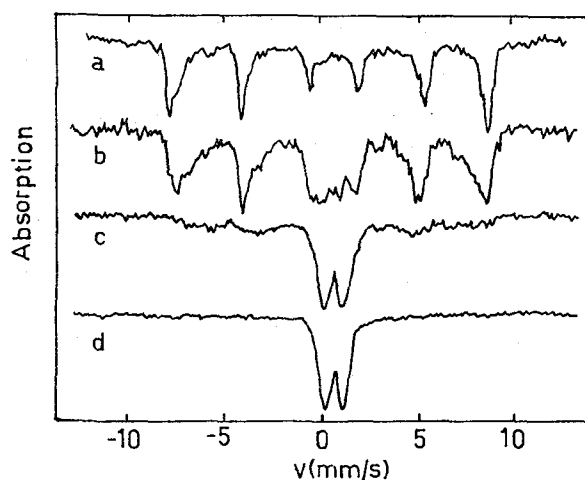


FIG. 12. — Mössbauer spectra of alkali borate glasses at room temperature. The  $\text{Fe}_2\text{O}_3$  concentrations in mole % are a) 24.2, b) 16.9, c) 13.9 and d) 11.4 (from ref. [46]).

about 5 mole % the iron is homogeneously dispersed and the magnetic interactions are weak. In such circumstances the ferric ion may show a broadened spectrum because the time for spin-spin or spin-lattice relaxation becomes comparable to the Larmor precession time [53]. At low temperatures, complete paramagnetic hyperfine splitting may appear if the iron is sufficiently dilute. Gusakovskaya *et al.* [113] recently deduced that the spin-lattice relaxation time decreased by a factor of two on passing from glass to crystal, and attributed the effect to changes in interatomic distances. No such effects will be observable for the ferrous ion using the Mössbauer effect because spin-lattice relaxation times are much too short. Between about 5 mole % and the solubility limit for iron in the glass, the magnetic and Mössbauer properties may resemble those of superparamagnetic particles in spite of the fact that there is no X-ray evidence for the existence of microcrystalline precipitates. The situation is probably akin to the critical superparamagnetism found in diamagnetically substituted iron oxides [114], and the existence of well defined iron

clusters should not necessarily be inferred. At the solubility limit, well defined microcrystallites of iron oxides or ferrites [115] such as  $\text{NaFeO}_2$  [43] begin to appear, and normal magnetic or superparamagnetic behaviour is found. Further references to work on microcrystalline precipitates are to be found in reference [43], but it should be remarked that all the magnetic properties of a glass, and particularly those due to phase separation are extremely sensitive to heat treatment and preparation method.

The spectrum of amorphous materials in the magnetically ordered state generally shows no quadrupole shift although the paramagnetic spectrum is frequently a well-separated doublet (Fig. 12). Bukrey *et al.* were led by this observation to suggest that paramagnetic doublet was actually a relaxation spectrum and they cast doubt on the reliability of using the doublet as an indicator of iron coordination number (§ 2.2.1). These doubts seem ill-founded. In the first place there is no inconsistency between a paramagnetic quadrupole doublet and lack of quadrupole shift in the ordered phase as there is generally no relation between the direction of the electric field gradient, which fluctuates from site to site in an amorphous solid, and the magnetic axis. The effect of the quadrupole interaction is just to broaden all the lines in the magnetic hyperfine pattern equally. Secondly, the assignment of coordination number is made on the basis of isomer shift, which is unchanged by magnetic relaxation.

Iron has been examined as a dispersion in glasslike carbons [116] and the complex Mössbauer spectra have been interpreted in terms of isolated Fe and  $\text{Fe}^+$  atoms and Fe and  $\text{Fe}_3\text{C}$  clusters. The relative amounts of the various forms of iron depends on the preparation method and overall iron concentration. Magnetically ordered iron clusters and isolated ferric ions have also been found recently in a polymer cross-linked by a  $\text{FeCl}_3$ -pyridine complex [117].

In summary, although the oxide glasses show magnetic behaviour which can be usefully studied by the Mössbauer effect, they are not very suitable as model systems for testing theories of amorphous magnetism as the iron has a strong tendency to segregate in clusters when it is present in concentrations of order or greater than the percolation limit, the concentration at which long-range order may be expected to set in.

**3.2.2 Random solid solutions.** — Diamagnetically-substituted iron oxides have been investigated by a great many people. A partial list of references may be found in reference [114]. Their relevance to amorphous materials lies in the influence of the randomly varying number of neighbours on the magnetic properties, and the main results of this work will be briefly stated.

At iron concentrations  $x$  which are of order or greater than the percolation limit (roughly  $2/n$ , where  $n$

is the number of nearest-neighbour cation sites), the compound orders magnetically at sufficiently low temperatures. The critical concentration for long-range ordering would be exactly the percolation limit for strictly-nearest neighbour interactions.

At temperatures well below the magnetic ordering temperature, the Mössbauer spectrum is a hyperfine pattern with broadened lines. As a first approximation it may be considered as a superposition of subspectra arising from different nearest-neighbour environments. If the distribution of magnetic and non-magnetic ions is random, the probability of an iron having  $z$  magnetic neighbours is

$$P_n(z) = \frac{n!}{z!(n-z)!} x^z (1-x)^{n-z}. \quad (4)$$

Although each subspectrum may itself be broadened because of the possible distribution in the neighbours magnetic environments [118] or because of a distribution of electric field gradients, it is nevertheless possible in some circumstances (e. g.  $n < 6$ ) to resolve the subspectra [114, 119, 120] and thereby use the Mössbauer effect to verify if the cation distribution is really random. The magnetisation of iron in different nearest-neighbour environments has a different temperature dependence [118] and generally the magnetic line-broadening increases with increasing temperature. However even at  $T = 0$  there may be some line broadening because of different super-transferred hyperfine fields for different nearest-neighbour environments. A similar set of results appears when the Mössbauer probe is the diamagnetic ion, except that the hyperfine field measured is a transferred hyperfine field, proportional to the number of magnetic neighbours and the resolution of different magnetic environments is easier [119].

The most interesting, but most complex spectra are found in the critical region, close to the magnetic ordering temperature. These appear to be a superposition of paramagnetic central peaks and a magnetic hyperfine pattern whose lines are extremely broad. Experiments in applied fields have indicated that the central peak is due to critical superparamagnetism although there is no geometrical tendency towards clusters at the diamagnetic concentrations studied [114]. Interpretations of these spectra have also been advanced in terms of a distribution of ordering temperatures or slowed relaxation of individual spins. Altogether, there is a resemblance between the concentration or temperature dependence of the Mössbauer spectrum of iron in these materials and in the amorphous oxide glasses. Compare figures 12 and 13. This suggests that the variation in the number of interacting neighbours is determining the magnetic properties in both systems.

The spin structures in the diamagnetically substituted oxides, if collinear for  $x = 1$ , tend to remain collinear

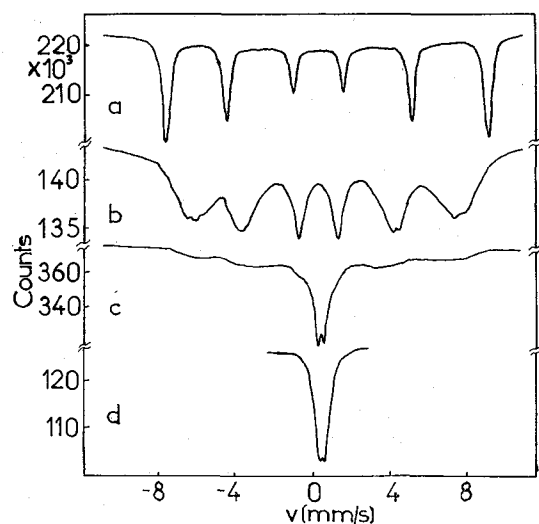


FIG. 13. — Mössbauer spectra of a diamagnetically substituted crystalline iron oxide ( $\text{Fe}_x\text{Rh}_{1-x}\text{O}_3$ ) at room temperature. The  $\text{Fe}_2\text{O}_3$  concentrations in mole % are a) 76, b) 54, c) 34 and d) 23 (from ref. [118]).

for somewhat smaller values of  $x$  as well. However, at values of  $x$  of order  $n_A J_{AA}/n_B J_{AB}$  in ferrites where the diamagnetic ions substitute on the B sublattice, canted spin structures begin to appear. A molecular field model has been developed for this random local canting [121], and the phenomenon has been well demonstrated by Mössbauer spectra in applied fields [122].

For values of  $x$  of order of the percolation limit, the probability  $P_n(0)$  of an iron ion having no magnetic nearest neighbours becomes appreciable. If only nearest-neighbour exchange applied, then there would appear a central paramagnetic peak whose intensity was proportional to  $P_n(0)$ , even at  $T = 0$ . In practice this has not been observed which suggests that either longer range exchange aligns these isolated ions at low temperatures, or else the solid solutions studied are so far from being random that there are no isolated iron ions. The former is the more likely explanation, and an implication is that the low-temperature susceptibility of the ordered amorphous antiferromagnet should not be dominated by these isolated magnetic ions.

3.2.3 *Amorphous iron compounds.* — Two sorts of nonmetallic amorphous iron compounds have been extensively studied by the Mössbauer effect, the ferrous halides [123] and ferric gels [95, 109].

In the crystalline form, the ferrous halides have widely differing Néel temperatures and hyperfine fields, the latter because the orbital and contact terms have different relative magnitudes and opposite signs. The amorphous halides, prepared by condensing a molecular beam on a cold ( $< 10$  K) substrate all have the same well-defined ordering temperatures at 21 K and almost the same hyperfine field. The results of Litterst *et al.* are summarised in Table III [123]. Spectra with different angles between the plane of the sample and the  $\gamma$ -direction showed that the direction of the hyperfine field was randomly oriented in the sample, and from the broad lines in the magnetically split spectrum a relative width of 25 % was derived for a Gaussian distribution of hyperfine fields. A Gaussian distribution of electric field gradient with a relative width of 20 % was derived from the spectra in the paramagnetic regime. The temperature-variation of the hyperfine field was much flatter than that calculated from any Brillouin function, and is in qualitative agreement with the theories of amorphous magnetism [102, 103]. These results are a vivid illustration of the sensitivity of magnetic order to crystal structure. The crystalline chloride and bromide have a hexagonal layer structure whereas the structure of the fluoride is akin to that of rutile. The values of the quadrupole coupling suggest that all the amorphous halides have a local symmetry for the ferrous ion similar to that in  $\text{FeF}_2$ . The change from crystalline to amorphous  $\text{FeF}_2$  thus depresses the ordering temperature, as expected from most theories [124] but the change from crystalline to amorphous  $\text{FeBr}_2$  actually increases it, presumably due to the change in local symmetry. It would be of interest to know the magnetic structure of the ordered phase in these amorphous compounds.

Synthetic ferric oxyhydroxide gels were characterised by Okamoto *et al.* [95] using a variety of techniques including X-ray, magnetic and Mössbauer measurements. They suggested a quasi-amorphous structure based on an hexagonally close-packed oxygen lattice with ferric ions randomly distributed in the octahedral

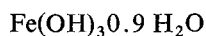
TABLE III

$^{57}\text{Fe}$  Data for Amorphous and Crystalline Ferrous Halides (ref. [123])

	$e^2 qQ$ (mm/s)	Amorphous $H_{\text{eff}} (T = 0)$ (kOe)	$T_c$ (k)	$e^2 qQ$ (mm/s)	Crystalline $H_{\text{eff}}$ (kOe)	$T_c$ (k)
$\text{FeF}_2$	5.3	(-) 165	21	5.7	- 329	78
$\text{FeCl}_2$	5.3	(-) 140	21	2.0	+ 3	24
$\text{FeBr}_2$	4.8	(-) 140	21	1.9	+ 30	11

interstices. The gels are strongly magnetic, and the Mössbauer spectra indicated a supermagnetic blocking temperature near 77 K.

A natural gel of empirical composition



was studied by the present author, and the spin structure was determined in the ordered state [109]. The gel, amorphous in electron and X-ray diffraction was composed of particles of diameter  $\sim 40 \text{ \AA}$ . The iron was essentially paramagnetic above 100 K and between about 10 K and 100 K the particles behaved superparamagnetically, with a small moment of approximately 9 emu/g. Below the blocking temperature there was some remanence [93], and the iron was all magnetically ordered. The spectrum in figure 14b was

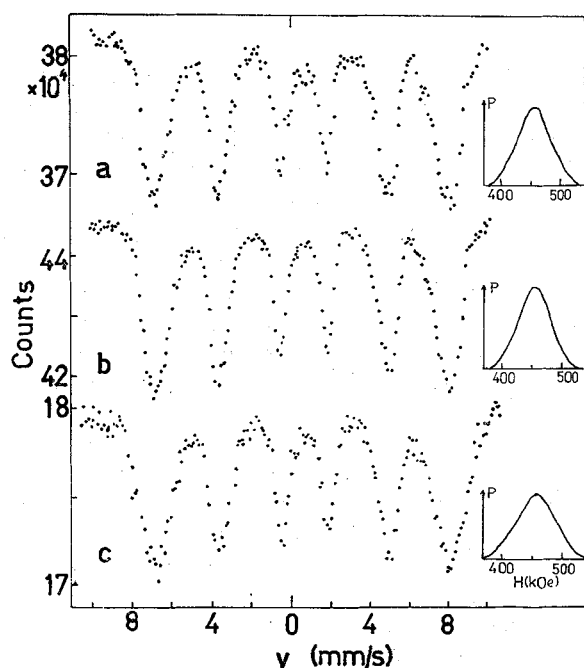


FIG. 14. — Mössbauer spectra of speromagnetic ferric gel at 4.2 K taken in an external field of a) 0 kOe, b) 10 kOe and c) 50 kOe parallel to the  $\gamma$ -direction. The insets show the hyperfine field distributions (from ref. [109]).

taken in a field of 10 kOe, sufficient to saturate the magnetic moment, whereas 50 kOe is more than enough to saturate it, and yet not enough to provoke a spin flop. The remarkable feature of these spectra is that there is no change in the relative intensities of the lines, which shows that the spin directions within a small particle are *randomly* oriented relative to the applied field, despite the saturation of their resultant moment. This can hardly be explained by single-ion anisotropy, which is very small for the  $\text{Fe}^{3+}$  ion. It was suggested that the spin arrangement was speromagnetic. The resultant moment of a particle containing  $N$  spins should be  $\sqrt{N}$  (the random walk), and this was found to be in good agreement with observation.

The relative width of the hyperfine field distribution at 4.2 K is rather narrow, about 15 %. A similar value is found in the diamagnetically-substituted oxides at low temperatures, and it cannot be inferred that the nearest-neighbour environment of the iron is uniform. It is likely that the speromagnetism in this ferric gel arises in the same way as the randomly canted spin structures found in the diamagnetically-substituted ferrites.

3.3 ALLOYS. — The magnetic properties of a few amorphous ferromagnetic alloys have been studied. In  $\text{Fe}_{80}\text{P}_{12.5}\text{C}_{7.5}$ , Tsuei *et al.* [125] found a temperature dependence of the average hyperfine field which followed a Brillouin function for  $S = 1$  rather closely, with a relatively well-defined Curie point at 586 K, far below that of crystalline iron. The broad hyperfine spectra were fitted with five subspectra whose relative intensities were given by eq. (4) with  $n = 8$ . Some magnetic and quadrupole broadening of the lines was required for a fit, the latter being due to random angles between the local electric field gradient and the magnetic axis. In the similar alloys  $\text{Fe}_x\text{P}_{100-x}$ ,  $75.6 \leq x \leq 91.0$  the hyperfine field decreased with increasing phosphorus content at room temperature [126] but whether this is due to a reduction in saturation moment or just an effect of the reduction of the Curie temperature is unclear from the data which was only collected at one temperature. Some moment reduction is anticipated in these alloys if the phosphorus contributes electrons to the iron d-band.

The most complete study of amorphous magnetism in alloys using the Mössbauer technique to date is that of Sharon and Tsuei on the  $\text{Fe}_x\text{Pd}_{80-x}\text{P}_{20}$  system with  $13 \leq x \leq 44$  [127]. The alloys are all ferromagnetic glasses, prepared by quenching the liquid. The data, some of which is shown in figure 15, was fitted on the basis of a continuous asymmetric distribution of hyperfine fields defined by three parameters. The electronic state of iron was found to remain essentially constant throughout the composition range although there is a marked difference in magnetic properties for  $x \leq 25$ . In the high iron concentrations, as may be seen from figure 15, the temperature variation of the hyperfine field is in qualitative agreement with Hendrick's theory [102]. For dilute iron concentrations, there is still magnetic order at sufficiently low temperatures, thought to be produced by a weak long-range interaction via the conduction electrons, by analogy with  $\text{AuFe}$ . Furthermore, the resistivity minimum found in quite concentrated alloys was attributed to spin-flip scattering by those irons subject to low hyperfine fields in the tail of the distribution.

The other class of amorphous alloy which has been investigated using Mössbauer spectroscopy, so far just on the iron, is the type  $\text{RFe}_2$  where R is Tb, Dy, Mo or Er [128]. The structure of these alloys is a random close packing of the iron and rare earth, and the strong local crystal field model of Harris *et al.* was proposed

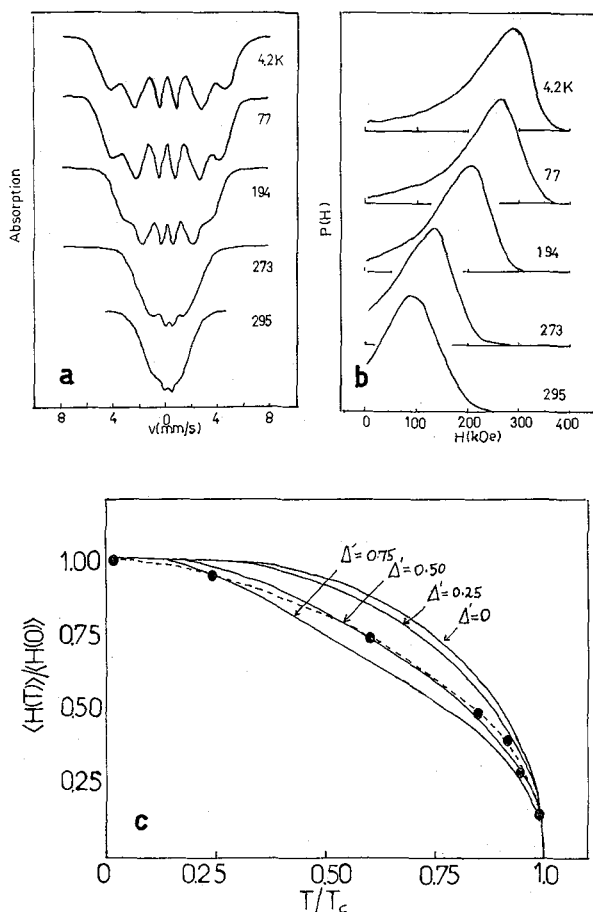


FIG. 15. — *a*) Mössbauer spectra of the amorphous ferromagnetic alloy  $\text{Fe}_{44}\text{Pd}_{36}\text{P}_{20}$  at various temperatures *b*) the corresponding hyperfine field distributions and *c*) the temperature variation of the reduced hyperfine field, compared with the theory of ref. [102] (eq. (3)) for several relative widths of the molecular field distributions (from ref. [127]).

to explain their magnetic properties [110] (§ 3.1). In the paramagnetic state the iron spectrum is a quadrupole doublet, both in the amorphous and crystalline forms, with a splitting of 0.6 mm/s. The amorphous alloys have a lower Curie temperature than the crystalline forms. Amorphous  $\text{TbFe}_2$  orders magnetically between 145 and 230 K whereas the crystalline form is ordered up to 612 K. The spectrum at 145 K was found to be flat, within the statistics and the authors suggest that the result might be explained by an electric field gradient of varying direction or else an extremely broad hyperfine field distribution. The published data is inadequate support for any such conclusions however. In the iron-phosphorous alloys [125-127]. A randomly varying electric field gradient direction was found to broaden the lines in the magnetic spectrum at 4.2 K, but it can be difficult to distinguish between broadening from this cause and broadening due to a distribution of iron moments or hyperfine fields.

It would be interesting to look at the Dy resonance in amorphous  $\text{DyFe}_2$ , for example, to verify strong crystal field model.

**4. Conclusions.** — This review allows some conclusions to be drawn about the scope and utility of the Mössbauer effect as a tool for examining the amorphous solid state. Four areas in which the technique might be expected to make some contribution can be defined, namely electronic processes, structure and bonding, phase transitions and magnetism. These four areas are listed in order of increasing importance from the point of view of a Mössbauer specialist, but an amorphous generalist might rank them in just the opposite order.

It is clear that the electronic processes occurring in amorphous solids are of the greatest theoretical and technical interest, and it is just as clear that the Mössbauer effect, essentially a microscopic probe, is unlikely to make much contribution towards understanding them. An exception might be charge transfer processes of the type  $\text{Fe}^{2+} \leftrightarrow \text{Fe}^{3+}$  which occur in some oxide glasses.

In principle, the Mössbauer effect should be a good technique for studying structure and bonding because the hyperfine interactions are essentially determined by the atom's local environment, and the nearest-neighbour configuration is the basic element in an amorphous structure. In practice, as the work reviewed here shown, it is rare that one can make unqualified deductions from the spectra. Usually the best that can be done is to make negative or qualitative statements like « the symmetry has changed on passing from the amorphous to the crystalline phase » ; « the structure is not microcrystalline » ; « the tin is not bound to arsenic » ; « the bonding is more ionic in the glass than in the crystal ». For instance, it is only with iron in the oxide glasses that one can infer the coordination number from the spectra. Even for tin, it is unclear whether there are 4 or 6 selenium neighbours in the As-Se-Sn glasses. Nevertheless, in the present state of knowledge of amorphous structures, the qualitative information currently obtainable by Mössbauer spectroscopy can be quite valuable, and may limit or permit a choice between possible model structures. Sometimes, however, it is impossible to exploit the isomer shift and quadrupole interaction to the maximum because the resonance has a poor energy resolution, or because the necessary background of systematic work is lacking. Notable efforts have been made with  $^{57}\text{Fe}$ ,  $^{119}\text{Sn}$ , and  $^{125}\text{Te}$ . The  $^{129\text{m}}\text{Te}$  source experiments look particularly promising.

So far as the glass transition is concerned, the Mössbauer effect has proved to be an excellent tool for investigating both the atomic or molecular vibration amplitudes and diffusion on a microscopic level. Experiments performed by scattering are not restricted to the usual Mössbauer elements. Also the possibility of using the effect to separate elastic and inelastic scattered radiation with a high energy resolution might find an application in general structural studies.

The area in which Mössbauer spectroscopy is likely to contribute most to our knowledge of non-crystalline



solids is their magnetic properties. The resolution of magnetic hyperfine interactions of iron or the rare-earths is sufficient, but not too good for a detailed knowledge of the distribution of magnetisation to be obtained. Particularly in the non-ferromagnetic structures the technique should prove invaluable both for discovering new spin structures such as speromagnetism, for measuring the temperature variation of the

atomic moment and for following the effect of the local environments on the atomic moments or zero-point spin deviations.

**Acknowledgments.** — The author wishes to thank C. Jeandey and H. Daver for the FeGe data, and R. Alben for reading part of the manuscript. He is grateful to G. M. Kalvius for a preprint of his review.

#### References

- [1] MOTT, N. F. and DAVIES, E. A., *Electronic Processes in Non-Crystalline Materials* (Oxford University Press) 1971, p. 194.
- [2] TURNBULL, D., *Contemp. Physics* **10** (1969) 473.
- [3] KALVIUS, G. M., Lectures at the «International Summer School on Frontier Problems in Nuclear and Solid State Physics», Predeal, Romania, September 1973.
- [4] RUBY, S. L., *J. Non-Cryst. Solids* **8-10** (1972) 78.
- [5] TANEJA, S. P., KIMBALL, C. W. and SHAFFER, J. C., *Mössbauer Effect Methodology* **8** (1973) 41.
- [6] KURKJIAN, C. R., *J. Non-Cryst. Solids* **3** (1970) 157.
- [7] RUBY, S. L., in *Perspectives in Mössbauer Spectroscopy*, Cohen, S. G. and Pasternak, M. (editors) (Plenum) 1973, p. 181.
- DEZSI, I., *Proceedings of the Conference on Mössbauer Spectroscopy* (Dresden) 1971, p. 77.
- [8] HOBSON, M. C., *Prog. Surface Membrane Science* **5** (1972) 1; *Adv. Colloid Interface Science* **3** (1971) 1.
- [9] WALKER, J. C., GUARNIERI, C. R. and SEMPER, R., *A. I. P. Conference Proceedings* **10** (1973) 1539.
- [10] *Amorphous and Liquid Semiconductors*, Tauc, J. (editor) (Plenum) 1974.
- [11] *Amorphous and Liquid Semiconductors*, Stuke, J. and Brenig, W. (editors) (Taylor and Francis) 1974, 2 vv.
- [12] *Tetraedrally Bonded Amorphous Semiconductors*, A. I. P. Conference Proceedings **20** (1974).
- [13] Structures Métalliques Désordonnées. *J. Physique* **35** Colloq. C4 (1974).
- [14] *Amorphous Magnetism*, Hooper, H. O. and de Graaf, A. M. (editors) (Plenum) 1973.
- [15] ZACHARIASEN, W. H., *J. Am. Chem. Soc.* **54** (1932) 3841.
- [16] VALENKOV, N. and PORAI-KOSHITS, E., *Z. Krist* **95** (1937) 195.
- [17] KREBS, H., *J. Non-Cryst. Solids* **1** (1969) 455.
- [18] SAYERS, D. E., LYTE, W. E. and STERN, E. A., in ref. [11] p. 403.
- [19] MOSS, S. C. in ref. [10] p. 17.
- [20] GRIGOROVICI, R. and MANAILA, R., *J. Non-Cryst. Solids* **1** (1969) 371.
- [21] POLK, D. E., *J. Non-Cryst. Solids* **5** (1971) 365.
- [22] GRIGOROVICI, R., in ref. [10] p. 45.
- [23] BERNAL, J. D., *Proc. R. Soc. A* **280** (1964) 299.
- [24] GOKULARATHNAM, C. V., *J. Mater. Sci.* **9** (1974) 673; DIXIMIER, J., in ref. [13] p. 11.
- [25] TAUC, J., in ref. [10] p. 159.
- [26] FRITZSCHE, H., in ref. [10] p. 313.
- [27] OVSHINSKY, S., *Phys. Rev. Lett.* **21** (1968) 1450.
- [28] DEB, S. K., *Phil. Mag.* **27** (1973) 801.
- [29] CARGILL, G. S., CHAUDHARI, P., CUOMO, J. J. and GAMBINO, R. J., *IBM J. Res. Dev.* **17** (1973) 66.
- [30] CZYZEK, G., FORD, J. L. C., LOVE, J. C., OBENSHAIN, F. E. and WEGENER, H. H. F., *Phys. Rev. Lett.* **18** (1967) 529.
- [31] RAGHAVAN, R. S. and PFEIFFER, L., *Phys. Rev. Lett.* **32** (1974) 512; *J. Physique* **35** (1974) C6-203.
- [32] O'CONNOR, D. A. in *Perspectives in Mössbauer Spectroscopy*, Cohen, S. G. and Pasternak, M. (editors) (Plenum) 1973, p. 171.
- [33] CHAMPENEY, D. C. and SEDGWICK, D. F., *Chem. Phys. Lett.* **15** (1972) 377; *J. Phys. C* **5** (1972) 1903.
- [34] SIMOPOULOS, A., WICKMAN, H., KOSTIKAS, A. and PETRIDES, D., *Chem. Phys. Lett.* **7** (1970) 615; REICH, S. and MICHAELI, I., *J. Chem. Phys.* **56** (1972) 2350.
- [35] ALBANESE, G. and GHEZZI, C., *Phys. Stat. Sol.* **a 22** (1974) 209.
- [36] POLLAK, H., De COSTER, M. and AMELINCKX, S., in *Mössbauer Effect*, Compton, D. M. J. and Schoen, D. (editors) (Wiley) 1962, p. 298.
- [37] PARGAMIN, L., LUPIS, C. H. P. and FLINN, P. A., *Met. Trans.* **3** (1972) 2093.
- [38] BHAT, V. K., MANNING, C. R. and BOWEN, L. H., *J. Amer. Ceram. Soc.* **56** (1973) 459.
- [39] FRISCHAT, G. H. and TOMANDL, G., *Glastechn. Ber.* **42** (1969) 182.
- [40] KURKJIAN, C. R. and SIGETY, E. A., *Phys. Chem. Glasses* **9** (1968) 73.
- [41] BELYUSTIN, A. A., OSTANEVICH, Y. M., PISAREVSKII, A. M., TOMILOV, S. B., BAI-SHI, U. and CHER, L., *Sov. Phys. Solid State* **7** (1965) 1163.
- [42] GOSSELIN, J. P., SHIMONY, U., GRODZINS, L. and COOPER, A. R., *Phys. Chem. Glasses* **8** (1967) 56.
- [43] COLLINS, D. W. and MULAY, L. N., *J. Amer. Ceram. Soc.* **54** (1971) 69.
- [44] LABAR, C. and GIELEN, P., *J. Non-Cryst. Solids* **13** (1973) 107.
- [45] LEWIS, G. K. and DRICKAMER, H. G., *J. Chem. Phys.* **49** (1968) 3785.
- [46] BUKREY, R. R., KENEALY, P. F., BEARD, G. B. and HOOPER, H. O., *Phys. Rev.* **B 9** (1974) 1052.
- [47] TARAGIN, M. F. and EISENSTEIN, J. C., *J. Non-Cryst. Solids* **3** (1970) 311.
- [48] HIRAYAMA, C., CASTLE, J. G. and KURIYAMA, M., *Phys. Chem. Glasses* **9** (1968) 109.
- [49] TARAGIN, M. F., EISENSTEIN, J. C. and HELLER, W., *Phys. Chem. Glasses* **13** (1972) 149.
- [50] SIN, G. K., KOSTIKAS, A. and YONG, S. M., *J. Korean Phys. Soc.* **5** (1972) 29.
- [51] SITHARAMARAO, D. N. and DUNCAN, J. P., *Rev. Chim. Min.* **9** (1972) 543.
- [52] VARNEK, V. A., VEREVKIN, G. V. and SOKOLOVA, V. K., *Inorg. Materials* **9** (1973) 662.
- [53] FRISCHAT, G. H. and TOMANDL, G., *Glastechn. Ber.* **44** (1971) 173.
- [54] ANDERSON, R. A. and MACCRONE, R. K., *J. Non-Cryst. Solids* **14** (1974) 112.
- [55] BRYUKHANOV, V. A., GOLDANSKII, V. I., DELYAGIN, N. N., KORYTKO, L. A., MAKAROV, E. F., SUZDALEV, I. P. and SHPINEL, V. S., *Sov. Phys. JETP* **16** (1963) 321.
- [56] GENDLER, T. S., MITROFANOV, K. P., PLOTNIKOVA, M. V., TYKACHINSKII, I. D. and FEDOROVSKII, Y. A., *Inorg. Materials* **7** (1966) 1091.
- [57] MITROFANOV, K. P. and SIDOROV, T. A., *Sov. Phys. Solid State* **9** (1967) 693.
- [58] BARTENEV, G. M., BREKHOVSKIKH, S. M., VARISOV, A. Z., LANDA, L. M. and TSYGANOV, A. D., *Sov. Phys. Solid State* **12** (1970) 972.
- [59] BARTENEV, G. M., SUZDALEV, I. P. and TSYGANOV, A. D., *Phys. Stat. Sol.* **37** (1970) 73.

- [60] BARTENEV, G. M., GOROKHOVSKII, V. A., TSYGANOV, A. D., SHCHERBAKOVA, V. P. and OVCHINNIKOV, A. I., *Inorg. Materials* **8** (1972) 1934.
- [61] UHRICH, D. L. and BARNES, R. G., *Phys. Chem. Glasses* **9** (1968) 184.
- [62] TARAGIN, M. F. and EISENSTEIN, J. C., *Phys. Rev. B* **2** (1970) 3490; *J. Non-Cryst. Solids* **11** (1973) 395.
- [63] VAIVAD, A. Y., VEITS, B. N., GRIGALIS, V. Y., DOMBROVSKA, Y. K., KONSTAT, Z. A., LISIN, Y. D. and TAKSAR, I. M., *Izvest Akad Nauk Latv SSSR. Ser. Khim* (1969) 504.
- [64] BLUME, N. A. and FELDMAN, C., *Solid State Commun.* **15** (1974) 965; BLUME, N. A., *J. Physique* **35** (1974) C6-401.
- [65] BOOLCHAND, P., HENNEBERGER, T. and OBERSCHMIDT, J., *Phys. Rev. Lett.* **30** (1973) 1292.
- [66] CHAUDHARI, P. and GRACZYK, J., *Non-Cryst. Solids* **14** (1974); ALBEN, R. and BOUTRON, P. (to be published).
- [67] BOOLCHAND, P., TRIPLETT, B. B., HANNA, S. S. and de NEUFVILLE, J. P., *Mössbauer Effect Methodology* **9** (1974).
- [68] BIENENSTOCK, A., in ref. [11] p. 49.
- [69] TSUEI, C. C. and KANKELEIT, E., *Phys. Rev.* **162** (1967) 312.
- [70] HAFEMEISTER, D. and de WAARD, H., *J. Appl. Phys.* **43** (1972) 5205.
- [71] SHENOY, G. K., FRIEDT, J. M., MALETTA, H. and RUBY, S. L., *Mössbauer Effect Methodology* **9** (1974).
- [72] BOOLCHAND, P., *Solid State Commun.* **12** (1973) 753; HENNEBERGER, T. and BOOLCHAND, P., *ibid.* **13** (1973) 1619.
- [73] BOOLCHAND, P., TRIPLETT, B. B., HANNA, S. S. and GROSSE, P., *J. Physique* **35** (1974) C6-227.
- [74] SEREGIN, P. P., SAGATOV, M. A., NASREDINOV, F. S. and VASILEV, L. N., *Sov. Phys. Solid State* **15** (1973) 1291.
- [75] SEREGIN, P. P., VASILEV, L. N. and BORISOVA, Z. U., *Inorganic Materials* **8** (1972) 493.
- [76] SEREGIN, P. P. and VASILEV, L. N., *Inorganic Materials* **8** (1972) 1238.
- [77] RENNINGER, A. L. and AVERBACH, B. L., *Phys. Rev.* **B 8** (1973) 1507.
- [78] VASILEV, L. N., SEREGIN, P. P. and SHIPATOV, V. T., *Inorganic Materials* **7** (1971) 1841.
- [79] BARTENEV, G. M., TSYGANOV, A. D., DEMBOVSKII, S. A. and MIKHAILOV, V. I., *J. Struct. Chem.* **12** (1970) 853.
- [80] BORISOVA, Z. U., VASILEV, L. N., SEREGIN, P. P. and SHIPATOV, V. T., *Soviet Physics-Semiconductors* **4** (1970) 443.
- [81] TANEJA, S. P., DWIGHT, A. E., GILBERT, L., HARPER, W. C., KIMBALL, C. W. and WOOD, C., *Phys. Chem. Glasses* **13** (1972) 153.
- [82] SAGATOV, M. A., BOLTAKS, B. I., VASILEV, L. N. and SEREGIN, P. P., *Sov. Phys. Solid State* **16** (1974) 297.
- [83] SEREGIN, P. P. and VASILEV, L. N., *Sov. Phys. Solid State* **14** (1972) 1325.
- [84] SEREGIN, P. P. and VASILEV, L. N., *Sov. Phys. Solid State* **13** (1972) 2258.
- [85] LONG, G. C., STEVENS, J. G. and BOWEN, L. H., *Inorg. Nucl. Chem. Lett.* **5** (1969) 799.
- [86] LONG, G. C., STEVENS, J. G., BOWEN, L. H. and RUBY, S. L., *Inorg. Nucl. Chem. Lett.* **5** (1969) 21.
- [87] RUBY, S. L., GILBERT, L. R. and WOOD, C., *Phys. Lett.* **37A** (1971) 453.
- [88] KIRIANOV, A. P., SAMARSKII, Y. A., ALEKSEEVSKII, N. E. and TSEBRO, V. I., *Proceedings of the Conference on the Applications of the Mössbauer Effect* (Tihany 1969) Akademiai Kiado, Budapest 1971, p. 313.
- [89] BOGOMOLOV, V. N., KLUSHIN, N. A. and SEREGIN, P. P., *Sov. Phys. Solid State* **14** (1973) 1729.
- [90] DAVER, H., MASSENET, O. and CHAKRAVERTY, B. K., in ref. [11] p. 1053.
- [91] MUIR, A. H., HOUSLEY, R. M., GRANT, R. W., ABDEL-GAWAD, M. and BLANDER, M., *Science* **167** (1970) 688.
- [92] MARZOLF, J. G., DEHN, J. T. and SALMON, J. F., *Adv. Chem.* **68** (1967).
- [93] COEY, J. M. D. and READMAN, P. W., *Earth Planetary Sci. Lett.* **21** (1973) 45.
- [94] COEY, J. M. D., SCHINDLER, D. W. and WEBER, P., *Can J. Earth Sci.* **11** (1974); COEY, J. M. D., *Geochem. et Cosmochim. Acta* **38** (1974).
- [95] OKAMOTO, S., SEKIZAWA, H. and OKAMOTO, S. I., in *Reactivity of Solids* (Chapman and Hall) 1972, p. 341.
- [96] VAN DER GIESSEN, A. A., *Philips Res. Repts. Suppl.* **12** (1968).
- [97] COLEMAN, M. F., DUNCAN, J. F. and SITHARAMARAO, D. N., *Rev. Chim. Min.* **7** (1970) 1129.
- [98] MACKENZIE, K. J. D., *Clay Minerals* **8** (1969) 161.
- [99] JANOT, C. and DELCROIX, P., *J. Physique* **35** (1974) C6-501. BOUCHEZ, R., COEY, J. M. D., COUSSEMENT, R., SCHMIDT, K. P., VAN ROSSUM, M., APRAHAMIAN, J. and DESHAYES, J., *J. Physique* **35** (1974) C6-541. EISSA, N. A., SALLAM, H. A. and KESZTHELYI, L., *J. Physique* **35** (1974) C6-569.
- [100] GUBANOV, A. I., *Sov. Phys. Solid State* **2** (1961) 468.
- [101] TSUEI, C. C., in ref. [14] p. 299.
- [102] HANDRICH, K., *Phys. Stat. Sol.* **32** (1969) K 55.
- [103] SIMPSON, A. W., *Phys. Stat. Sol.* **40** (1970) 207.
- [104] HASEGAWA, R., *Phys. Stat. Sol.* **b 44** (1971) 613.
- [105] SIMPSON, A. W., *Wiss. Zeit. dTU Dresden* **3** (1974).
- [106] TAHIR KHELL, R. A., *Phys. Stat. Sol.* **b 63** (1974) K 95.
- [107] EGAMI, T., SACLII, O. A., SIMPSON, A. W., TERRY, A. L. and WEDGWOOD, F. A., *J. Phys. C* **5** (1972) L 261.
- [108] SIMPSON, A. W. and BRAMBLEY, D. R., *Phys. Stat. Sol.* **a 49** (1972) 685.
- [109] COEY, J. M. D. and READMAN, P. W., *Nature* **246** (1973) 476.
- [110] HARRIS, R., PLISCHKE, M. and ZUCKERMANN, M. J., *Phys. Rev. Lett.* **31** (1973) 160.
- [111] HOOPER, H. O., *A. I. P. Conference Proceedings* **10** (1973) 702.
- [112] MATHER, G. R., HOOPER, H. O., KENEALY, P. F. and BUKREY, R. R., *A. I. P. Conference Proceedings* **5** (1972) 821.
- [113] GUSAKOVSKAYA, I. G., LARKINA, T. I. and GOLDANSKII, V. I., *Sov. Phys. Solid State* **14** (1973) 2274.
- [114] COEY, J. M. D., *Phys. Rev.* **B 6** (1972) 3240.
- [115] SHAW, R. R. and HEASLEY, J. H., *J. Amer. Ceram. Soc.* **50** (1967) 297.
- [116] THOMPSON, A. W., WALKER, P. L. and MULAY, L. N., in ref. [14] p. 111; YAJIMA and OMORI, M., *Chem. Lett.* (1974) 277.
- [117] MEYER, C. and PINERI, M., *J. Polymer. Sci.* (to be published).
- [118] COEY, J. M. D. and SAWATZKY, G. A., *Phys. Sol. Stat.* **b 44** (1971) 673; *J. Phys. C* **4** (1971) 2386.
- [119] LYUBUTIN, I. S. and VISHNYAKOV, Y. S., *Phys. Stat. Sol.* **a 12** (1972) 47.
- [120] LYUBUTIN, I. S., DODOKIN, A. P. and BELYAEV, L. M., *Kristallografiya* **18** (1973) 992.
- [121] ROSENCAWIG, A., *Can. J. Phys.* **48** (1970) 2857; 2868.
- [122] PETITT, G. A. and FORESTER, D. W., *Phys. Rev.* **B 4** (1971) 3912; LEUNG, L. K., EVANS, B. J. and MORRISH, A. H., *Phys. Rev.* **B 8** (1973) 29; PETITT, G. A., *Solid State Commun.* **13** (1973) 1611; CLARK, P. E. and MORRISH, A. H., *Phys. Stat. Sol.* **a 19** (1973) 687.
- [123] BOYLE, A. J. F., KALVIUS, G. M., GRUEN, D. M., CLIFTON, J. R. and MCBETH, R. L., *J. Physique* **32** (1971) C1-224; LITTERST, F. J., KALVIUS, G. M. and BOYLE, A. J. F., *A. I. P. Conference Proceedings* **18** (1974) 616.
- [124] HANDRICH, K., *Sov. Phys. JETP* **37** (1973) 703.
- [125] TSUEI, C. C., LONGWORTH, G. and LIN, S. C. H., *Phys. Rev.* **170** (1968) 603.
- [126] BONDER, V. V., POVITSKII, V. A. and MAKAROV, Y. F., *Fiz. Metal. Metalloved.* **30** (1970) 1061.
- [127] SHARON, T. E. and TSUEI, C. C., *Phys. Rev.* **B 5** (1972) 1047.
- [128] SARKAR, D., SEGNAN, R. and CLARK, A. E., *AIP Conference Proceedings* **18** (1974) 636; SARKAR, D., SEGNAN, R., CORNELL, E. K., CALLEN, E., HARRIS, A., PLISCHKE, M. and ZUCKERMANN, M. J., *Phys. Rev. Lett.* **32** (1974) 542.
- [129] TRICKER, M. J., THOMAS, J. M., OMAR, M. H., OSMAN, A. and BISMAY, A., *J. Mater. Sci.* **9** (1974) 1115.